Title: Using the three dimensional shape of plant cells to predict probabilities of cell division orientation

Short title (50 characters): Predicting division planes using cell shape

Pablo Martinez[1,2,5], Lindy A. Allsman[1,5], Kenneth A. Brakke[3], Christopher Hoyt[4], Jordan Hayes[5], Carolyn G. Rasmussen[1,5*]

1 Center for Plant Cell Biology, Department of Botany and Plant Sciences, University of California, Riverside
2 Biochemistry and Molecular Biology Graduate Program, University of California, Riverside
3 Department of Mathematics, Susquehanna University, Lancaster PA
4 Center for Plant Cell Biology NSF-REU, Harvey Mudd College
5 Institute of Integrative Genome Biology

CGR ORC-ID 0000-0002-4354-6295
PM ORC-ID 0000-0003-4846-4958
LAA ORC-ID 0000-0002-0190-9086

*Correspondence to carolyn.rasmussen@ucr.edu

Author contributions:

PM assembled figures; PM, LAA, CH, CGR performed experiments, JH and CH contributed new methods and tools, KAB developed Surface Evolver and contributed new methods and tools, CGR supervised the experiments, PM and CGR wrote the paper with comments from all authors.

Abstract

Cell division is essential for the growth of any organism. One aspect of cell division that plays a critical role in growth and development in multicellular organisms is the orientation of the division plane. Proper establishment of the division plane significantly contributes to normal organization of the plant body. One critical limitation to understanding division plane orientation lies in separating cell shape cues from mechanical or developmental regulation. We developed a probabilistic three-dimensional (3D) model of plant cell division that relies only on 3D cell shape, which allows us to quantitatively assess and separate the contribution of cell shape from other factors. One factor, four-way junction avoidance, in which plant cells place new walls so that they are offset from the existing walls of their neighbors, was demonstrated using this model. At a population level, the division predictions accurately predicted ~95% of in vivo cell divisions.

Introduction

Cell division planes are dictated by geometric, mechanical and polarity cues in plants, animals, bacteria, and fungi (1). A challenging problem in understanding division plane orientation lies in separating the effects of cell polarity or mechanical cues from the effects of cell-shape mediated cues. In plant and animal cells, the absence of polarity or mechanical cues leads to the default division plane, which bisects the long axis of the cell (1, 2). In zebrafish embryos, the placement of future divisions can be inferred by cell shapes created by the previous divisions: at a population level these changes are driven by cell-cell interactions (3). In the late 1800's, biologists identified basic patterns of plant cell division. Hofmeister showed that the plane of division was typically perpendicular to the primary growth axis (4). Sachs observed that a new cell wall often formed at a 90 degree angle to the mother cell wall and split the cell in two equal volumes (5). Errera suggested that cell divisions closely mimicked soap films, often preferring the smallest local plane to minimize the surface area of the division (6). Errera's interpretation was later simplified to the smallest global division plane that divided the cell into two equal parts. Over-simplification from multiple local to single global division plane significantly weakened the predictive properties of Errera's rules to account for the observed stochasticity in division plane orientation, leading biologists to ignore this problem for decades (2).

Recently, researchers have used computational or mathematical approaches to understand plant cell division plane orientation in 2 dimensions (2D) (7–9). In several studies, empirically derived factors were added to account for the stochasticity of division orientations observed. In the freshwater green alga *Coleochaete scutata*, cell division typically follows the shape of the cells, but a "stochastic parameter" was used to produce the correct proportion of divisions in the anticlinal and periclinal orientations (10). Anticlinal divisions occur perpendicular to the surface of the tissue while periclinal divisions occur parallel to the surface of the tissue (schematic cell with typical division orientations outlined in Fig. S1A). Similarly, Besson and Dumais used cells from algae, trichomes of the core-eudicot venus flytrap, fern, and *Zinnia elegans* to predict division plane orientations (11). The difference in lengths between two predicted divisions, with addition of an empirically defined stochasticity factor, was sufficient to describe the relative proportions of these two predicted division lengths in a population across distantly related plant species. Several other 2D approaches did not include stochasticity factors. In isotropically growing *Arabidopsis thaliana* shoot apical meristem cells, the shortest path through the center of mass of the cell best fit observations, although it did not reflect the variability of in vivo cell sizes (9). Finally, a fitness function that combined new cell wall length minimum with area equalization, was generated to accurately predict division planes in *A. thaliana* meristems and functioned similarly to “modern” Errera predictions (12).

Plant cell divisions that do not follow geometry-based rules generally undergo precisely controlled asymmetric divisions which have critical functions in development (13–17). In the case where cells divide symmetrically, there are examples when cells divide with an increased probability along a longer plane rather than the shortest plane. Cells under mechanical stress divided along the axis of principal stress even if it did not coincide with the the shortest division plane geometrically (18). Division planes parallel to tissue level stress were generated either by curvature or by differential growth in *A. thaliana* shoot apical meristem boundary cells (19). A significant population of tobacco cultured cells (BY-2) divided longitudinally after plasmolysis, potentially due to release of mechanical tension along the longitudinal axis of the cell (20).

An interest in 3D cell division modeling led to division plane analysis in the *A. thaliana* embryo (17, 21). The center of mass for each cell was used as a point to sample 2000 different planes to identify the lowest flat surface area. Some embryonic cells did not divide according to the shortest plane, but instead divided asymmetrically to produce unequal daughter cell volumes. Asymmetric divisions in the embryo were driven by response to auxin and associated with alterations in both gene expression and differentiation. Mutants that do not respond to auxin lost division asymmetry in these cells (22). Although this approach elegantly predicted a potential global minimum in 3D, it did not provide a probabilistic prediction.

We used a 3D mathematical modeling approach to generate a probabilistic division plane prediction for any cell. This model depends only on the shape of the cell: divisions are performed by initiating soap-film-like area-minimizing gradient descent from multiple starting planes. Because these probabilities are calculated completely independently of microtubule dynamics, mechanical stresses or other cell interactions, purely geometric contributions can be fully separated from mechanical or developmental inputs. We used this model to demonstrate that PPBs, microtubule and microfilament structures that accurately predict the future division plane in typical land plant cells (23–27), closely match the predicted division planes unless a four-way junction is present.

Results and Discussion

We established a geometry-based model to generate predicted local minimum divisions for any cell shape using Surface Evolver (28). Micrographs of maize cells with PPBs were taken with 0.2 micron Z-stacks (Fig. 1A shows a single Z-plane). The images were semi-automatically thresholded and their 3-dimensional (3D) surfaces were extracted (Fig. 1B). The surfaces were imported into Surface Evolver (Fig. 1C). The surfaces were smoothed using 30th degree spherical harmonics, a method which approximates the cell outline as a function of polar coordinate angles (29) (Fig. 1D). Higher or lower degrees of spherical harmonics were inaccurate or caused errors in later steps, respectively (Fig. S2A-B, Table S1, supplementary materials and methods). Reproducibility tests indicated variation in volume <10% and ~0.5% variability in division plane predictions (standard error measurement, Fig. S3, TABLE S2).

Mathematically predicted divisions were generated for each of the cells. First, a set of 241 starting planes which evenly sampled the entire cell volume was used to initiate a process known as gradient descent. Gradient descent iteratively minimized the surface area until the lowest surface area was reached while maintaining equal volume and ensuring that the division surface met the mother-cell cortex at a right angle (Fig. 1E-J, Movie S1).

After gradient descent was completed for each of the 241 starting planes, 241 predicted divisions were produced to divide the cell into two equal volumes, but only a few local minima in the cell were specified. In other words, many of the division predictions from one cell had almost the same surface area (average coefficient of variance = 0.6 %, n = 87) and the same location in the cell. The YFP-TUBULIN signal was used to reconstruct the PPB in 3D (Fig. 1K-L). The location of the PPB was aligned with the predicted surface (Fig. 1M-N, PPB offset measurements are described below). The predicted divisions which settled at the same local minimum in the cell were offset 1.375 +/- 0.1598 μm^2 (average +/- SEM) from each other relative to the midplane of the PPB. The PPBs used in this dataset were typically ~2 µm in width so these predicted division planes would lie within the PPB. Because these predictions specified the same local minima in the cell, they were grouped into four symmetric division categories based on their surface area and their location within the cell: transverse, longitudinal, periclinal and other (Fig. 2 A,B, and as illustrated schematically in Fig. S1A).

Aspects of cell shape that alter division plane prediction probabilities

For each cell analyzed, the probability of predicting each division category varied depending on cell shape features. All cells had transverse division predictions, potentially because it is the simplest division that likely also generates a global minimum surface area. In ~11% of cells analyzed, only a transverse division was predicted (Fig. S4A). When these cells were observed for special features, their cell shapes had more irregularities. To quantify this, the regularity of cell shape defined by an “abnormality” index, was generated for each cell. Abnormality was defined by the ratio of the area surface center and the volume center for the cell. Cells with a low abnormality index (more “normal”) usually have fewer protrusions while those with a higher abnormality index (less “normal”) have more protrusions that contribute to the surface area. Cells that had only transverse division predictions (n=9) had significantly a higher abnormality index than those with two or more predicted divisions (n=78, Fig S4A. Mann-Whitney *P* =0.0015).

This initial observation suggested that cell shape could either facilitate or prevent certain division predictions. One shape cue is the corner of the cell, a local maximum that potentially inhibited further gradient descent. Corners therefore promoted division predictions along non-transverse axes. Lack of a well defined corner or straight edge (cell wall) perpendicular to the division plane was observed in cells when a longitudinal or periclinal division was not predicted. In cells with only predicted transverse and periclinal divisions (~12%, n = 10) there was a lack of a straight edge along the y-plane to stabilize a longitudinal prediction (Fig. S4B). There were ~19% of cells which had only transverse and longitudinal predicted divisions due to lack of edges in the z-plane that could stabilize a periclinal division (Fig. S4C). Alternatively, longitudinal or periclinal division predictions were prevented by lack of two parallel walls perpendicular to the division plane. Cells with predicted transverse, longitudinal, and periclinal divisions (~36%) made up the largest group (Fig. S4D). An additional group of cells (~22%) had predictions for all canonical symmetric division categories and an additional category we called “other”, as shown (Fig. 2A and 2B). As the number of division categories predicted increased, the abnormality index decreased, suggesting that cells with well-defined features (as opposed to irregular features and lack of cell edges) were more likely to predict additional division categories (Fig. S5A).

While transverse and longitudinal divisions are readily observed in the epidermal layer of a developing maize leaf no “other” or periclinal divisions were observed in this in vivo dataset. This is consistent with their overall low prediction probabilities, at 1% and 0.8% at a population level, respectively. While rare, examples like the crescent shaped “other” predicted divisions (Fig. 2A and B) have been observed in other datasets while imaging dividing maize leaf cells (Fig. S6A-D). In contrast, periclinal divisions were much more rare in vivo than predicted in silico. In over 1000 dividing maize epidermal cells across several developmental stages and samples, only one epidermal periclinal division was observed. Periclinal divisions are observed in other cell layers in the developing maize leaf, associated with vasculature formation (30) or other developmental processes (31–33). Since periclinal divisions are not observed in vivo but are predicted based on the geometry of the cell, there may be molecular or mechanical mechanisms which inhibit the cell’s ability to initiate a periclinal division.

Cell shape was correlated with PPB location - Prolate cell shapes resulted in more transverse predictions

Since the cells imaged had transverse and longitudinal PPBs, we compared the features of these two types of cells. Cells with longitudinal PPBs displayed significantly higher proportions of predicted longitudinal divisions compared to those with a transverse PPB (11.2% vs 5.4%, Mann-Whitney, *P* = 0.0004, Fig. 3A, other division categories shown in Fig. S7A-C). We assessed whether a feature of the cell shape promoted higher proportions of longitudinal predictions in cells that formed longitudinal PPBs. First, we assessed whether there was any difference in abnormality index between the two cell categories. Cells with longitudinal (n=10) and transverse (n=76) PPBs did not have significantly different abnormality indices (Fig. S5B, Mann-Whitney, *P* = 0.36). To measure shape differences between cells with longitudinal or transverse PPBs using a metric independent of cell size, we compared the ratio of the largest and smallest eigenvalues. The eigenvalues were determined by three eigenvectors calculated from the moment of inertia matrix for each cell. Cells with lower eigenvalue ratios were more cube-shaped, while cells with higher ratios tended to be long and thin or prolate (Fig. 3B). On average, cells with transverse PPBs (average eigenvalue ratio = 6.3, n=76) had larger eigenvalue ratios compared to cells with longitudinal PPBs (average eigenvalue ratio = 5.1, n=10) indicating that their shape was more prolate (Mann-Whitney, *P* = 0.03, Fig. 3C). The ratio of eigenvalues were plotted as a function of percent transverse predicted: long and thin cells had more transverse division predictions (Fig. 3D). Cells with smaller eigenvalue ratios had higher proportions of non-transverse division predictions in silico and also have higher frequencies of longitudinal PPBs in vivo. Because this was similar to observations from the landmark Besson and Dumais (BD) 2D probabilistic model (8), we used a 3D version of the BD model to calculate the probabilities of divisions. The BD model underestimated the number of non-transverse divisions predicted, potentially due to differences inherent in the transition between 2 and 3D or due to the long and thin maize cells imaged compared to the more square cells used to calculate the BD stochasticity factor (Supplementary Materials and Methods, Fig. S8).

Accuracy and deviations of predicted divisions compared to PPB location: 4-way junction avoidance

The predicted divisions were compared to the observed location of the PPB. We assessed how well the PPB and predicted division overlapped by measuring the distance in μm^2 between the midplane of the PPB and the cortical region of the predicted division, which we refer to as PPB offset. If the offset between the PPB and the predicted division was low, the midplane of the PPB and the surface of the predicted division were close to each other. In almost all cases, the location of the PPB was close to one of the predicted divisions. The PPB offset was $0.38\mu m^2$ +/- 0.46 (S.D., n = 52) for cells whose PPB placement had no neighboring cell influence (Fig. 4A-C). The PPB offset was similar for transverse and longitudinally placed PPBs (Fig. S9). This indicates that a cell, without any influence from its neighbors, accurately and precisely forms the PPB along a predicted division plane.

Significant deviations in PPB location from predicted divisions were also observed. In cases when cells had high offset between the PPB midplane and the predicted division (Fig 4A, average $3.85\mu m^2$ +/- 1.43 S.D., n=32), the large offset occurred at a three-way junction, where an adjacent cell wall met the precise region where the division was predicted; shown in a schematic cell (Fig. S1B) and examples seen in vivo (Fig. 4D-E). In other words, the PPB location was offset from the mathematically optimal division plane to avoid creating a four-way junction. Avoidance of four-way junctions is a recognized feature of plant cells (34) to increase structural stability. Elegant microscopy showed that both the phragmosome (35) and the PPBs (21) in adjacent cells do not overlap. However, it was not known whether these PPBs simply followed the geometric constraints of the cell or whether they were shifted away from the geometrically predicted division plane. Alterations in PPB location away from an adjacent wall strongly suggests that a signal, whether chemical, mechanical or both, is communicated between cells to avoid a four-way junction.

PPB Dynamics and Modeling: PPBs avoid adjacent PPBs and sometimes switch orientation

PPB avoidance of four-way junctions prompted us to determine how PPB microtubules responded to adjacent cell walls using time-lapse imaging. In one example, the PPB appeared in two different locations in the cell, split over a region containing a three-way-junction (Fig. 5A, Movie S2), which then resolved into one PPB. The PPB moved over time, settling close to the predicted division (with an offset of 1.8 μm^2) over a time-period of ~2 hours. In several other examples, the PPB was split into two PPBs by two adjacent cell walls (Fig. 5B and 5C). These double PPBs resolved in several different ways. Either one of the PPBs disappeared before metaphase (Fig. 5B-5C, Movie S2-S3) or both PPBs disappeared in metaphase, but the end result was a single straight cell wall that matched the location of one of the PPBs. Double PPBs were not resolved via creation of an oblique division that connected both former PPB sites and maintained equal volume of the resulting daughter cells, as observed for tobacco cultured cells (BY-2) (36),(37). The final new cell wall (division plane) of cells with double PPBs indicated that, in these maize cells, four-way junction avoidance overrides the principle of equal volume daughter cells. We did not observe enough double PPBs in time-lapse to determine whether the PPB chosen was typically closer to or further from the geometrically predicted division. Examples of both closer (Fig. 5B, offset = 4.9 μm^2, Movie S3) and further (Fig. 5C, offset = 6.93 μm^2, Movie S4) final division locations were observed compared to the optimal predicted divisions.

In addition to PPB avoidance of adjacent cell walls, PPBs in neighboring cells also avoided each other. This observation is consistent with Azolla root-cell PPBs that do not overlap with PPBs in neighboring cells (38). Live-cell imaging was used to determine how cells establish their division site when two neighboring PPBs are adjacent to each other. We hypothesized that a cell which enters mitosis first will establish a division close to the mathematically predicted division while the neighboring cell entering mitosis later would be offset to prevent forming a future four-way junction. However, PPB offset was not determined by the relative timing of neighbor cell mitotic entry. Examples include a cell in a late G2 whose PPB offsets the neighboring PPB of cell earlier in G2 (Fig. 6A, Movie S5), a cell in early G2 whose PPB offsets the PPB of a neighboring cell in later G2 (Fig. 6B, Movie S6), and a cell that entered mitosis had a more offset final division location compared to the cell which entered mitosis later (Fig. 6C, Movie S7). Therefore, the signal that promotes PPB offset is established well before the PPB narrows. Combining this with observations that most PPBs closely match the location of the geometrically predicted division (Fig. 4A), we speculate that the signal to prevent future four-way junctions between neighboring cells must be transient.

Predictions on a population level account for ~95% of in vivo divisions

The population of cells imaged were from young maize adaxial leaf epidermal cells with a ligule height around 2 mm, had 88.5% (n=77/87) transverse PPBs and 11.5% (n=10/87) longitudinal PPBs. The mathematically predicted divisions using Surface Evolver for this population were 92.2% transverse, 6% longitudinal, 1% periclinal and 0.8% other. ~95% of the in-vivo divisions probabilistically match those predicted by the model. There was no significant difference in transverse and longitudinal divisions predicted by the model compared to in vivo observations, although there were almost twice as many observed longitudinal divisions in vivo (6% in silico vs 11.5% in vivo, chi-squared, P = 0.3012). This suggests that cell shape is a significant contributor to division plane orientation. Rarely (n = 2 in ~100 cases), we observed PPB orientation switch in vivo from both transverse to longitudinal (Fig. S10A, Movie S8) and longitudinal to transverse (Fig. S10B, Movie S9). Therefore, the division site specified by the PPB may rarely switch orientation, even until late G2. However, this is unlikely to meaningfully contribute to the overall population-level division orientations specified by the PPB. Although not observed in this dataset, it is likely that other factors, such as mechanical (19) or developmental regulation (17, 39) would alter probabilities of division orientation from solely geometrically predicted divisions.

Conclusion

This probabilistic predictor of division plane orientation in 3D is an important step forward because it provides a method to predict division based only on cell shape, allowing dissection of the relative contributions of shape as opposed to mechanical or developmental regulation. Overprediction of periclinal divisions by the model suggest that division plant orientation is not determined by cell shape cues alone. Indeed, periclinal divisions are known to be tightly regulated and occur only in specific developmental stages (30–32, 40).

This model does not provide a mechanism to describe how the plant cell establishes the division in response to cell shape. In plants, the cortical microtubule array has a complex interaction with the cell wall and can indirectly alter cell shapes (41–44). Defects in cortical microtubule organization often lead to altered cell wall placement resulting in aberrantly shaped daughter cells (45–49). Localized microtubule stabilization promotes organization of cortical microtubule arrays to specific orientations, which can be later used to determine the orientation of the PPB and the division site of a cell (50). Intriguingly, our data showed that PPB orientation can spontaneously shift. To our knowledge, the only examples showing division orientation shifting occurred after response to mechanical pressure, wounding or neighbor cell ablation (18, 35, 51–53) . In terms of analyzing mutants with aberrant division plane orientation, it is challenging to determine whether PPB placement defects arise as a consequence of altered cell shape or the absence of protein function. This model will provide insight into whether mutant cells have PPBs that align with predicted division planes based on their geometry to untangle cell shape defects from division plane specification defects.

Materials and Methods

Young maize leaf epidermal cells were chosen from a 28-day-old plant expressing a live cell marker for microtubules. Maize leaves were dissected to reveal symmetrically dividing cells (54). Cell walls were stained with propidium iodide or identified using the microtubule marker, YFP-TUBULIN (55). The adaxial side of a leaf with a ligule height ~2 mm was imaged directly above the ligule towards the leaf margin. The cell volumes were imported into Surface Evolver, and smoothed using spherical harmonics. Next, 241 uniformly distributed starting planes were used to initiate gradient descent to generate 241 division predictions. These were categorized based on their location in the cell. Each predicted division was compared to the PPB midline (PPB offset). When time-lapse imaging was performed according to previously described conditions (23, 56). Detailed methods can be found in supplementary materials.

Acknowledgments

We thank Professor Amir Moradifam (UCR) for pointing CGR to the research of Professor Ken Brakke. CH was supported by the National Science Foundation REU grant #1461297 to the UC-Riverside Center for Plant Cell Biology. CGR gratefully acknowledges NSF-MCB #1505848 and #1716972 and an UCR Office of Research Collaborative Seed Grant.

Figures

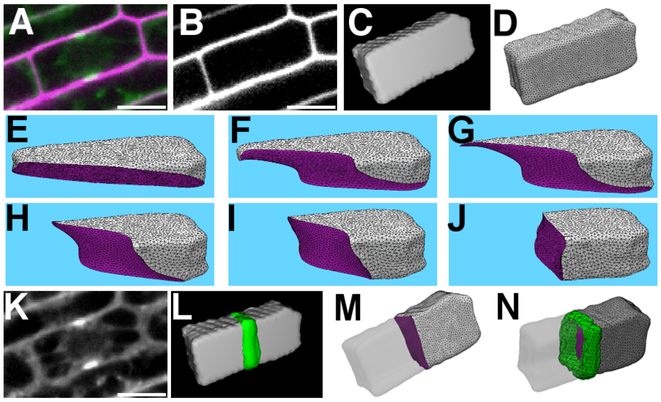
A
B
C
D
E
F
G
H
I
J
K
L
M
N

Figure 1: Method to generate division plane predictions. (A) Maize adaxial epidermal cell expressing YFP-TUBULIN (green) and stained with propidium iodide to outline cell walls (magenta). (B) Propidium iodide staining was used to (C) reconstruct the 3D surface. (D) Surface after 30 degree spherical harmonics in Surface Evolver. (E-J) An example of gradient descent from an initial starting position to a transverse division plane. (K) YFP-TUBULIN signal was used to (L) reconstruct the PPB (green). (M) The final division predicted by Surface Evolver was (N) overlaid with the PPB. Scale bar = 10μm.

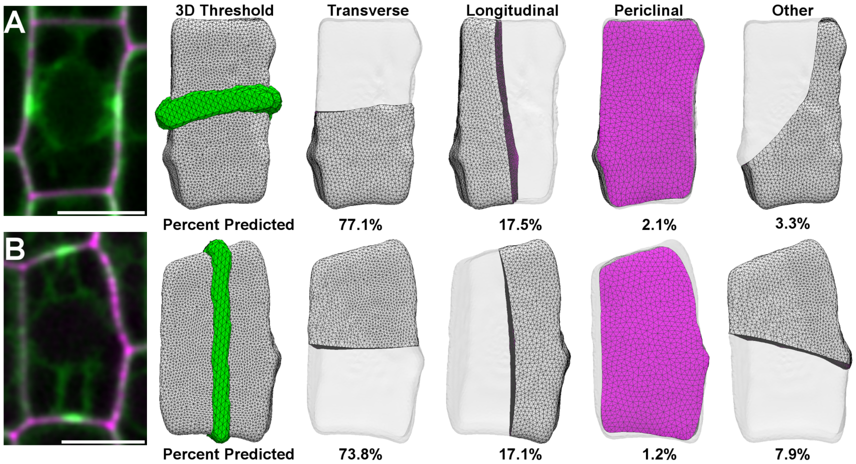
A
3D Threshold
Transverse
Longitudinal
Periclinal
Other
Percent Predicted
77.1%
17.5%
2.1%
3.3%
B
Percent Predicted
73.8%
17.1%
1.2%
7.9%

Figure 2: Representative cells in which modeling predicted all division categories, with percent predicted below each category. (A) Cell with a transverse PPB and examples of each division category. (B) Cell with a longitudinal PPB with the 3D reconstruction of the PPB overlaid on the surface of the cell with examples of each division category. Scale bar = 10μm.

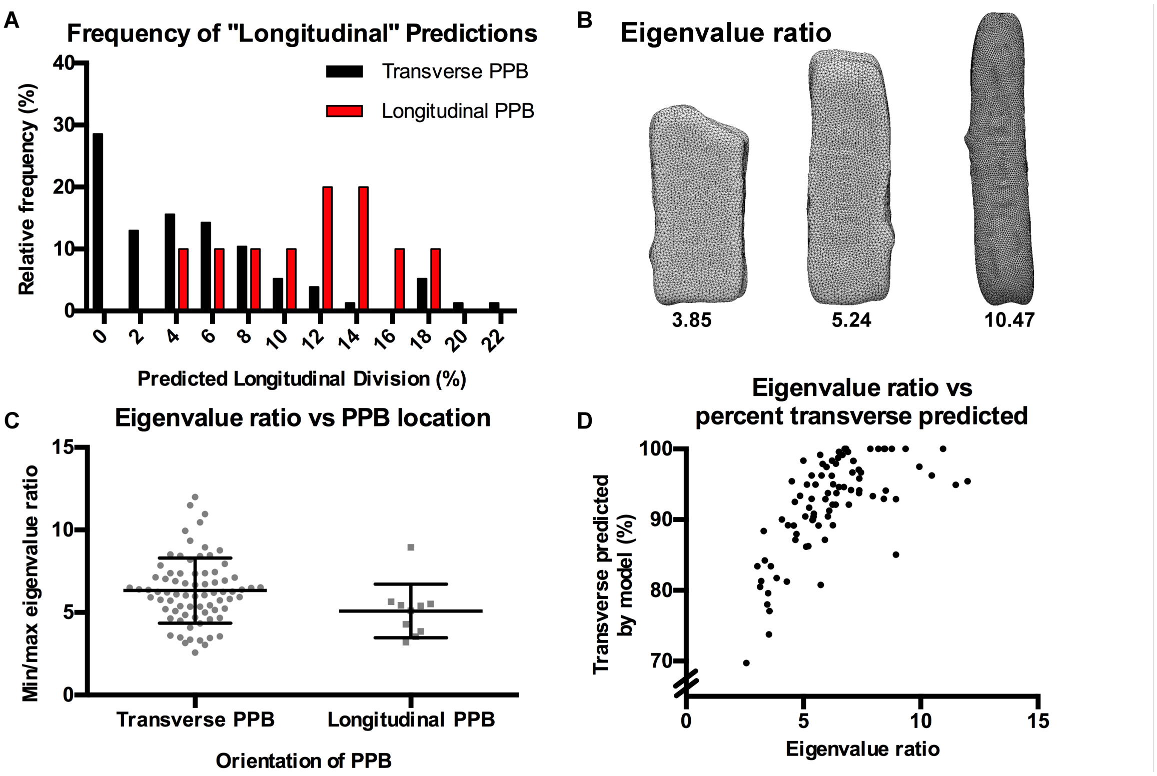

Figure 3: Cells with longitudinal PPBs are both more cube-shaped and also have more longitudinal predictions than cells with transverse PPBs. (A) Histogram of longitudinal predictions frequencies between cells with transverse (black) or longitudinal (red) PPBs. Cells with longitudinal PPBs predicted more longitudinal divisions than those with transverse PPBs (Mann-Whitney, *P* = .0005). (B) Cells with varying eigenvalue ratios. Larger eigenvalue ratios reflected longer and thinner cells. (Cells not displayed to scale). (C) Dot plot of eigenvalue ratios of cells with a transverse (n=76) or longitudinal PPB (n=10). Cells with transverse PPB had significantly higher eigenvalue ratios (Mann-Whitney, *P* = 0.0282). (D) Eigenvalue ratio versus percent transverse division predicted. Eigenvalue ratio and higher proportions of transverse divisions predicted were correlated (*P* = <.0001, Pearson r value = 0.6555).

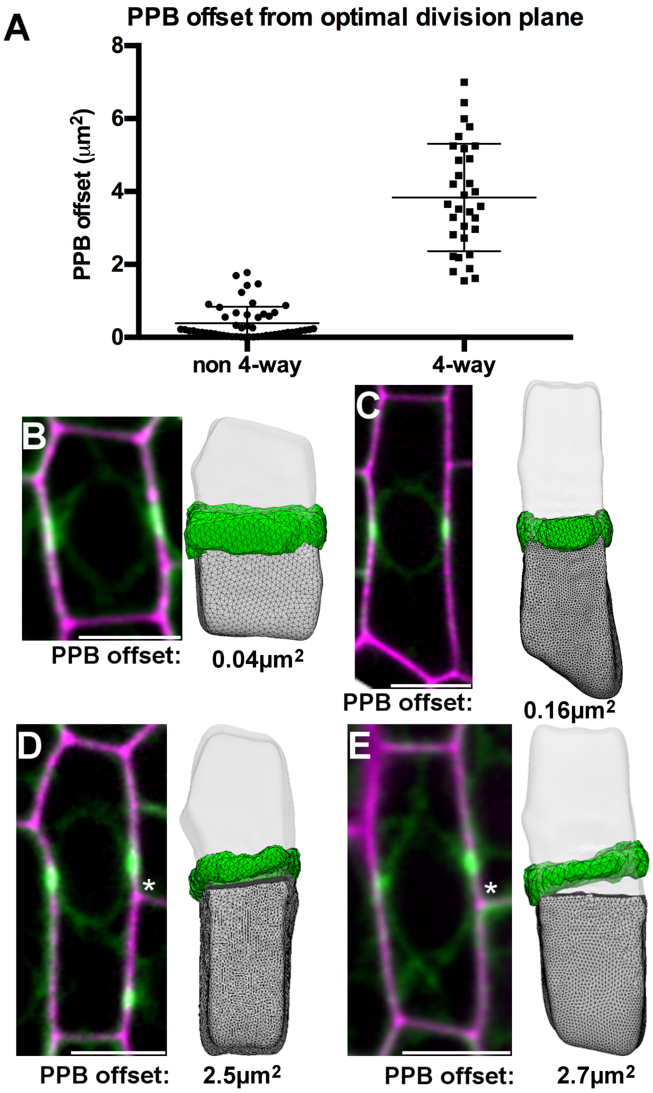

Figure 4: Comparison between predicted divisions and location of the PPB. (A) Accuracy of PPB placement was measured as the distance from the midplane of the PPB to the closest predicted division surface. Cells with (right) or without (left) four-way junction avoidance were analyzed separately. The PPB offset was 0.38µm^2 +/- 0.46 (S.D., n = 52) for cells whose PPB placement had no four-way junction avoidance, and was significantly higher for cells which avoided the creation of a four-way junction (average 3.85µm^2 +/- 1.43 S.D., n=32, Mann-Whitney *P* = < 0.0001). This indicates that a cell, without any influence from its neighbors, accurately and precisely forms the PPB along a predicted division plane. (B-E) Maize epidermal cells expressing YFP-TUBULIN (green) and stained with propidium iodide (magenta) and predictions with overlaid PPBs and PPB offset values indicated below. (B-C) Examples of cells with no four-way junction avoidance. (D-E) Example of cells with four-way junction avoidance and corresponding PPB offset. Neighboring cell walls are marked with an asterisk. Scale bar is 10µm.

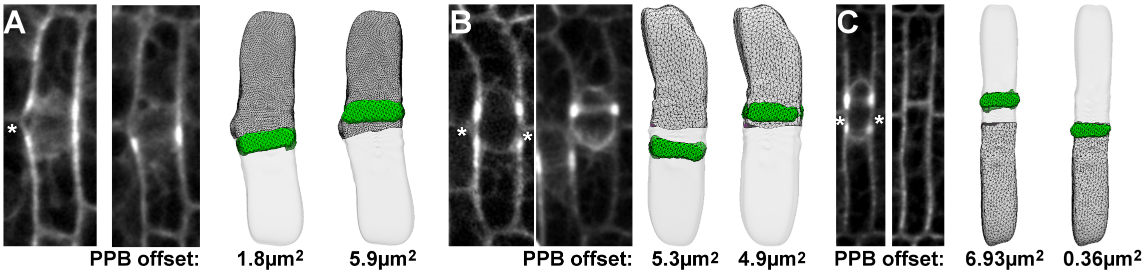

Figure 5. Live cell imaging of PPBs avoiding four-way junctions using maize cells expressing YFP-TUBULIN. Adjacent to timelapse images are cells with “best fit” predicted divisions and their PPB offset. (A) Time-lapse of a cell with a split PPB that merged into one PPB before entering mitosis. The final PPB location more closely matches the predicted division. (B) Time-lapse of a double PPB that was resolved into one PPB before entering mitosis. (C) Time-lapse of a cell which displayed a double PPB that never resolved and but completed division. Modeling of the cell shows that the final division site is further from the geometrically predicted division than the location of the other PPB. Neighboring cell walls indicated with an asterisk. Scale bar is 10µm.

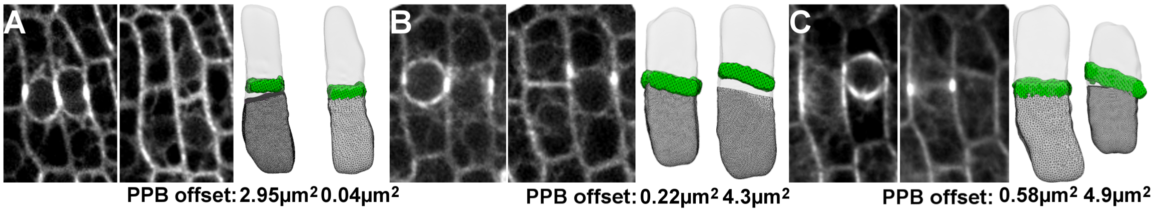

Figure 6. Live cell imaging of epidermal cells expressing YFP-TUBULIN to observe PPBs that avoid neighboring cell PPBs. To the right of the micrographs, are the results of modeling the cell and comparing the best fit predicted surface to each of the PPBs, shown with PPB offset below. (A) Time-lapse imaging of two neighboring dividing cells: these cells entered metaphase within 30 minutes of each other. The cell on the left, which was further along mitosis and finished telophase first, was offset by the cell on the right, which finished telophase later. (B) The cell on the left, which was further along in mitosis and had finished telophase, has a PPB which was not offset by the cell on the right, which was still in pre-prophase stage. (C) The cell on the right, which was further along mitosis and had finished telophase, was offset by the cell on the left, with a forming PPB. Scale bar is 10µm.

References

1. Minc N, Piel M (2012) Predicting division plane position and orientation. *Trends Cell Biol* 22(4):193–200.

2. Besson S, Dumais J (2014) Stochasticity in the symmetric division of plant cells: when the exceptions are the rule. *Front Plant Sci* 5. doi:10.3389/fpls.2014.00538.

3. Xiong F, et al. (2014) Interplay of Cell Shape and Division Orientation Promotes Robust Morphogenesis of Developing Epithelia. *Cell* 159(2):415–427.

4. Hofmeister W (1863) Zusatze und Berichtigungen zu den 1851 veroffentlichen Untersuchungengen der Entwicklung hoherer Kryptogamen. *Jahrbucher fur Wissenschaft und Botanik* 3:259–293.

5. Sachs J (1878) Uber die Anordnung der Zellen in jungsten Pflanzentheilen. *Arb Bot Inst Wurzburg* 2:46–104.

6. Errera L (1888) Über Zellformen und Siefenblasen. *Bot Cent.bl* 34:395–399.

7. Dupuy L, Mackenzie J, Haseloff J (2010) Coordination of plant cell division and expansion in a simple morphogenetic system. *Proceedings of the National Academy of Sciences* 107(6):2711–2716.

8. Besson S, Dumais J (2011) Universal rule for the symmetric division of plant cells. *Proc Natl Acad Sci U S A* 108(15):6294–6299.

9. Sahlin P, Jönsson H (2010) A modeling study on how cell division affects properties of epithelial tissues under isotropic growth. *PLoS One* 5(7):e11750.

10. Dupuy L, Mackenzie J, Haseloff J (2010) Coordination of plant cell division and expansion in a simple morphogenetic system. *Proc Natl Acad Sci U S A* 107(6):2711–2716.

11. Besson S, Dumais J (2011) Universal rule for the symmetric division of plant cells. *Proc Natl Acad Sci U S A* 108(15):6294–6299.

12. Shapiro BE, Tobin C, Mjolsness E, Meyerowitz EM (2015) Analysis of cell division patterns in the *Arabidopsis* shoot apical meristem. *Proc Natl Acad Sci U S A* 112(15):4815–4820.

13. De Smet I, Beeckman T (2011) Asymmetric cell division in land plants and algae: the driving force for differentiation. *Nat Rev Mol Cell Biol* 12(3):177–188.

14. van Dop M, Liao C-Y, Weijers D (02/2015) Control of oriented cell division in the Arabidopsis embryo. *Curr Opin Plant Biol* 23:25–30.

15. Rasmussen CG, Humphries JA, Smith LG (2011) Determination of symmetric and asymmetric division planes in plant cells. *Annu Rev Plant Biol* 62:387–409.

16. Kajala K, et al. (2014) Omics and modelling approaches for understanding regulation of asymmetric cell divisions in arabidopsis and other angiosperm plants. *Ann Bot* 113(7):1083–1105.

17. Yoshida S, et al. (2014) Genetic control of plant development by overriding a geometric division rule. *Dev Cell* 29(1):75–87.

18. Lintilhac PM, Vesecky TB (1981) Mechanical Stress and Cell Wall Orientation in Plants. II. The Application of Controlled Directional Stress to Growing Plants; with a Discussion on the Nature of the Wound Reaction. *Am J Bot* 68(9):1222.

19. Louveaux M, Julien J-D, Mirabet V, Boudaoud A, Hamant O (2016) Cell division plane orientation based on tensile stress in *Arabidopsis thaliana*. *Proceedings of the National Academy of Sciences* 113(30):E4294–E4303.

20. Asada T (2013) Division of shape-standardized tobacco cells reveals a limit to the occurrence of single-criterion-based selection of the plane of symmetric division. *Plant Cell Physiol* 54(6):827–837.

21. Gunning BE, Hardham AR, Hughes JE (1978) Evidence for initiation of microtubules in discrete regions of the cell cortex in Azolla root-tip cells, and an hypothesis on the development of cortical arrays of microtubules. *Planta* 143(2):161–179.

22. Yoshida S, et al. (2014) Genetic control of plant development by overriding a geometric division rule. *Dev Cell* 29(1):75–87.

23. Martinez P, Luo A, Sylvester A, Rasmussen CG (2017) Proper division plane orientation and mitotic progression together allow normal growth of maize. *Proc Natl Acad Sci U S A*. doi:10.1073/pnas.1619252114.

24. Rasmussen CG, Humphries JA, Smith LG (2011) Determination of symmetric and asymmetric division planes in plant cells. *Annu Rev Plant Biol* 62:387–409.

25. Pickett-Heaps JD, Northcote DH (1966) Organization of microtubules and endoplasmic reticulum during mitosis and cytokinesis in wheat meristems. *J Cell Sci* 1(1):109–120.

26. Camilleri C, et al. (2002) The Arabidopsis TONNEAU2 gene encodes a putative novel protein phosphatase 2A regulatory subunit essential for the control of the cortical cytoskeleton. *Plant Cell* 14(4):833–845.

27. Van Damme D, Vanstraelen M, Geelen D (2007) Cortical division zone establishment in plant cells. *Trends Plant Sci* 12(10):458–464.

28. Brakke K (1992) The Surface Evolver. *Exp Math* 1(2):141–165.

29. Givoli D (2004) High-order local non-reflecting boundary conditions: a review. *Wave Motion* 39(4):319–326.

30. Sakaguchi J, Fukuda H (2008) Cell differentiation in the longitudinal veins and formation of commissural veins in rice (Oryza sativa) and maize (Zea mays). *J Plant Res* 121(6):593–602.

31. Walbot V, Egger RL (2016) Pre-Meiotic Anther Development: Cell Fate Specification and Differentiation. *Annu Rev Plant Biol* 67:365–395.

32. Sylvester AW, Cande WZ, Freeling M (1990) Division and differentiation during

normal and liguleless-1 maize leaf development. *Development* 110(3):985–1000.

33. Poethig S (1984) Cellular parameters of leaf morphogenesis in maize and tobacco. *White, R, A,, Dickison, W, C ed (s) Contemporary problems in plant anatomy Academic Press: Orlando, etc*:235–259.

34. Flanders DJ, Rawlins DJ, Shaw PJ, Lloyd CW (1990) Nucleus-associated microtubules help determine the division plane of plant epidermal cells: avoidance of four-way junctions and the role of cell geometry. *J Cell Biol* 110(4):1111–1122.

35. Sinnott EW, Bloch R (1941) Division in Vacuolate Plant Cells. *Am J Bot* 28(3):225–232.

36. Hasezawa S, Sano T, Nagata T (1994) Oblique cell plate formation in tobacco BY-2 cells originates in double preprophase bands. *J Plant Res* 107(3):355–359.

37. Yoneda A (2005) Decision of Spindle Poles and Division Plane by Double Preprophase Bands in a BY-2 Cell Line Expressing GFP-Tubulin. *Plant Cell Physiol* 46(3):531–538.

38. Gunning BE, Hardham AR, Hughes JE (1978) Pre-prophase bands of microtubules in all categories of formative and proliferative cell division in Azolla roots. *Planta* 143(2):145–160.

39. De Rybel B, et al. (2014) Plant development. Integration of growth and patterning during vascular tissue formation in Arabidopsis. *Science* 345(6197):1255215.

40. Sheridan WF, Golubeva EA, Abrhamova LI, Golubovskaya IN (1999) The mac1 mutation alters the developmental fate of the hypodermal cells and their cellular progeny in the maize anther. *Genetics* 153(2):933–941.

41. Wasteneys GO, Ambrose JC (2009) Spatial organization of plant cortical microtubules: close encounters of the 2D kind. *Trends Cell Biol* 19(2):62–71.

42. Paredez AR, Persson S, Ehrhardt DW, Somerville CR (2008) Genetic evidence that cellulose synthase activity influences microtubule cortical array organization. *Plant Physiol* 147(4):1723–1734.

43. Zhu C, et al. (2015) The fragile Fiber1 kinesin contributes to cortical microtubule-mediated trafficking of cell wall components. *Plant Physiol* 167(3):780–792.

44. Li S, Lei L, Somerville CR, Gu Y (2012) Cellulose synthase interactive protein 1 (CSI1) links microtubules and cellulose synthase complexes. *Proc Natl Acad Sci U S A* 109(1):185–190.

45. Pietra S, et al. (2013) Arabidopsis SABRE and CLASP interact to stabilize cell division plane orientation and planar polarity. *Nat Commun* 4:2779.

46. Komis G, et al. (2017) Katanin Effects on Dynamics of Cortical Microtubules and Mitotic Arrays in Arabidopsis thaliana Revealed by Advanced Live-Cell Imaging. *Front Plant Sci* 8:866.

47. Kirik A, Ehrhardt DW, Kirik V (2012) TONNEAU2/FASS regulates the geometry of

microtubule nucleation and cortical array organization in interphase Arabidopsis cells. *Plant Cell* 24(3):1158–1170.

48. Hamant O, et al. (2008) Developmental patterning by mechanical signals in Arabidopsis. *Science* 322(5908):1650–1655.
49. Hashimoto T (2015) Microtubules in plants. *Arabidopsis Book* 13:e0179.
50. Kirik V, et al. (2007) CLASP localizes in two discrete patterns on cortical microtubules and is required for cell morphogenesis and cell division in Arabidopsis. *J Cell Sci* 120(24):4416–4425.
51. Heisler MG, et al. (2010) Alignment between PIN1 Polarity and Microtubule Orientation in the Shoot Apical Meristem Reveals a Tight Coupling between Morphogenesis and Auxin Transport. *PLoS Biol* 8(10):e1000516.
52. Hush JM, Overall RL (1996) Cortical microtubule reorientation in higher plants: dynamics and regulation. *J Microsc* 181(2):129–139.
53. Bringmann M, Bergmann DC (2017) Tissue-wide Mechanical Forces Influence the Polarity of Stomatal Stem Cells in Arabidopsis. *Curr Biol* 27(6):877–883.
54. Sylvester AW (2000) Division decisions and the spatial regulation of cytokinesis. *Curr Opin Plant Biol* 3(1):58–66.
55. Mohanty A, et al. (2009) Advancing cell biology and functional genomics in maize using fluorescent protein-tagged lines. *Plant Physiol* 149(2):601–605.
56. Rasmussen CG (2016) Using Live-Cell Markers in Maize to Analyze Cell Division Orientation and Timing. *Plant Cell Division*, Methods in Molecular Biology., ed Caillaud M-C (Springer New York, New York, NY), pp 209–225.
57. Wadsworth P (2012) Using cultured mammalian cells to study mitosis. *Cold Spring Harb Protoc* 2012(2):205–212.
58. Arganda-Carreras I, et al. (2016) *Trainable_Segmentation: Release v3.1.2* (Zenodo) doi:10.5281/zenodo.59290.